



Biological Screening Studies of DNA Relate Metal Complexes from Benzyldiene-4-imino-2,3-dimethyl-1-phenyl-3-pyrazolin-5-one and 2-aminothiazole

A. PALANIMURUGAN and A. KULANDAISAMY*

PG and Research Department of Chemistry, Raja Doraisingam Government Arts College, Sivagangai-630 561, India

*Corresponding author: E-mail: kulandai.kvn@gmail.com

Received: 13 September 2017;

Accepted: 18 October 2017;

Published online: 31 January 2018;

AJC-18751

Novel terdentate cationic complexes of Cu(II), Ni(II), Co(II), Mn(II) and Zn(II) ion have been prepared using a Schiff base derived from benzyldiene-4-imino-2,3-dimethyl-1-phenyl-3-pyrazolin-5-one and 2-aminothiazole. The structural features of metal-chelates have been confirmed by micro-analytical data, FAB-Mass spectra, powder XRD, SEM, FTIR, UV-visible, ¹H NMR, EPR, CV and thermal analysis techniques. The analytical data of the complexes correspond well with the general formula [ML₂]Cl₂. The high conductance data of metal chelates supports their 1:2 electrolytic nature. The magnetic susceptibility and electronic absorption spectra of the complexes indicate that all the metal-chelates exhibit octahedral geometry around the central metal ion. Powder XRD data and SEM images persist that the complexes are nano size grain with polycrystalline structure. DNA interaction studies of [CuL₂]Cl₂ complex have been done by electronic spectral and cyclic voltammetric measurements which revealed that the binding occurs through intercalation between complex and DNA interaction of [CuL₂]Cl₂ complex with CT-DNA leads to hypochromism. The MIC values against the growth of microorganisms are lower for metal chelates than the ligand. This is mainly due to lipophilicity of metal ion in complexes.

Keywords: Schiff base, Metal complexes, Cyclic voltammetry, EPR Spectra, DNA interaction, Antimicrobial activities.

INTRODUCTION

Now a day, a far-reaching number of works have been done on the transition metal Schiff base complexes derived from pyrazolone derivatives due to their potential applications in biological, pharmacological, clinical and analytical fields [1-4]. Among the pyrazolone derivatives, 4-Aminoantipyrine has two potential donor sites which have been further improved by condensing it with aldehydes, ketones, thiocarbazides and carbazides [5,6]. Aminothiazoles have the ability to act as primary amine and condensing it with 4-aminoantipyrine derivative and enhance tridentate to tetradentate [7,8]. The interaction of Schiff base metal complexes with DNA has gained much interest towards their applications as therapeutic agents. Transition metal ions are essential for the normal functioning of living organisms. Therefore, it is not surprising that transition metal complexes are of great interest as effective drugs and these complexes with tunable coordination environments and versatile spectral and electrochemical properties offer a great scope for design of new species that are suitable for DNA interactions [9-11]. The literature survey revealed that more attention has been given to Schiff base complexes derived by using 4-aminoantipyrine as a basic fundamental moiety. But no work has been reported on the condensation of such

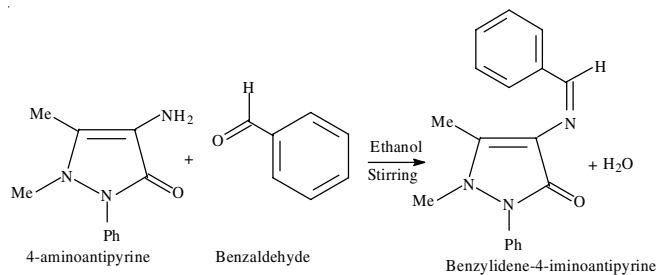
derivatives with 2-aminothiazole [12-20]. Hence, in this paper, we report herein the synthesis, characterization and biological investigations of Cu(II), Ni(II), Co(II), Mn(II) and Zn(II) metal complexes derived from benzyldiene-4-imino-2,3-dimethyl-1-phenyl-3-pyrazolin-5-one and 2-aminothiazole, which can utilized for biological screening activities and may consent the development of new drugs for the treatment of diseases.

EXPERIMENTAL

Benzaldehyde, 4-aminoantipyrine, 2-aminothiazole and all metal salts were purchased from Merck (Darmstadt, Germany). All the solvents used for spectroscopic and electrochemical studies which have purified by standard procedures [21,22]. CT-DNA was procured from Bangalore Genei (India). Agarose (molecular biology grade) and Ethidium bromide (EB) were obtained from Sigma-Aldrich (St. Louis, Missouri, USA). Tris(hydroxymethyl)aminomethane hydrochloride (Tris-HCl) buffer solution was prepared using deionized and double distilled water. Himedia chemicals were used as such for antimicrobial studies.

Elemental Analyzers (C, H and N) were carried out with an Elementar Vario EL III Carlo Erba 1108 analyzer and Fast atomic bombardment mass spectra (FAB-MS) were obtained

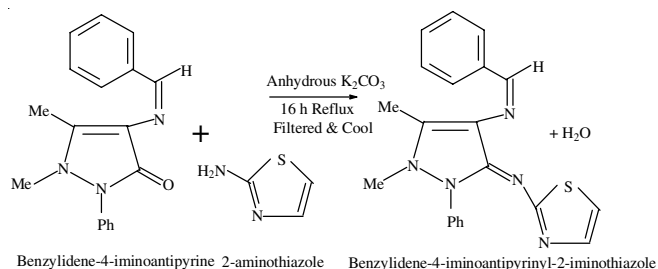
using a Mass Spectrometers Jeol SX-102 (FAB) in a 3-nitrobenzylalcohol matrix. The X-band ESR spectra of the copper complex in DMSO solution at 77 K were recorded on a JEOL 47 series ESR spectrometer at Sophisticated Analytical Instrumentation facility, IIT, Mumbai. ^1H NMR spectra (300 MHz) of the Schiff base and its zinc complex were recorded on a Bruker Advance DRX 300 FTNMR spectrometer using CDCl_3 as solvent (TMS used as internal standard). Powder XRD patterns (XPRT-PRO) and cyclic voltamogram were recorded at Alagappa University, Karaikudi. SEM was recorded under ultra high vacuum with AlK_{α} excitation at 250 W in Bharathidasan University, Trichy, India. For electrochemical measurements CHI 620C electrochemical analyzer was used. It contains three electrode systems; glassy carbon electrode as working electrode, platinum wire as auxiliary electrode and Ag/AgCl as reference electrode. Solutions were deoxygenated by purging with N_2 prior to measurements. Tetra butyl ammonium perchlorate was used as supporting electrolyte. Molar conductance of the chelates (10^{-3} M) was measured at room temperature using Deepvision Model-601 digital conductivity meter. Magnetic susceptibility measurements of chelates were carried out by employing Gouy balance at room temperature. $\text{CuSO}_4 \cdot 5\text{H}_2\text{O}$ was used as calibrant. The purity of Schiff base and its metal-chelates were checked by thin layer chromatography [23].



Scheme-I: Preparation of benzylidene-4-imino-2,3-dimethyl-1-phenyl-3-pyrazolin-5-one

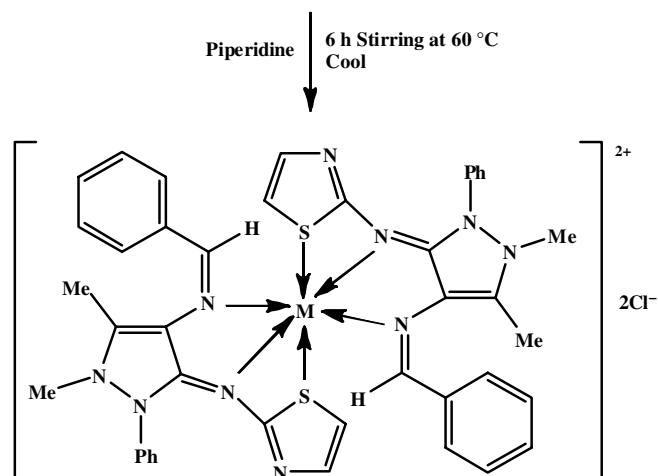
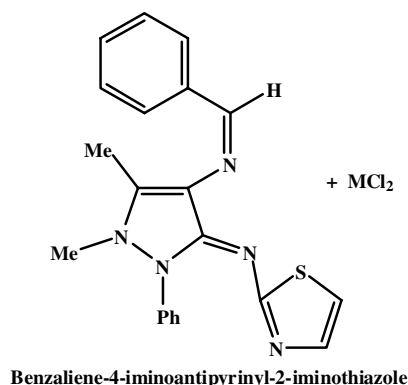
Synthesis of Schiff base (HL): An ethanolic solution (30 mL) of benzylidene-4-imino-2,3-dimethyl-1-phenyl-3-pyrazolin-5-one (10 mmol, 2.91 g) was refluxed with 2-aminothiazole (20 mmol, 2.002 g) in the presence of anhydrous K_2CO_3 (2 g) for about 16 h (**Scheme-II**). The resulting solution was filtered and the solvent was removed by evaporation in water bath. The red pasty mass obtained was stirred with 50 mL deionized water. The product obtained was filtered, washed with water and recrystallized in methanol.

Synthesis of metal chelates: An ethanolic solution (50 mL) of $\text{CuCl}_2/\text{NiCl}_2/\text{CoCl}_2/\text{MnCl}_2$ and ZnCl_2 (5 mmol) and Schiff



Scheme-II: Synthesis of benzylidene-4-imino-2,3-dimethyl-1-phenyl-3-pyrazolin-5-imino-2-thiazole

base (5 mmol) was boiled under reflux about 6 h (**Scheme-III**). The solvent was reduced to one third in water bath. The resultant solution was cooled and stirred with 10 mL of petroleum ether (40-60 $^\circ\text{C}$). The precipitated metal-chelates was filtered and recrystallized from methanol.



Scheme-III: Synthesis of Schiff base metal chelates; where, M = Cu(II)/Ni(II)/Co(II)/Mn(II) and Zn(II) ions

Antimicrobial assay: The synthesized Schiff base (HL) and its metal chelates were tested for their *in vitro* antimicrobial activity against two Gram-positive (*Staphylococcus aureus* and *Bacillus subtilis*) and three Gram-negative (*Escherichia coli*, *Klebsiella pneumonia* and *Salmonella typhi*) bacterial strains and for *in vitro* antifungal activity against *Candida albicans*, *Rhizoctonia bataticola*, *Aspergillus flavus*, *Aspergillus niger* and *Rhizopus stolonifer* by well diffusion method using nutrients agar as medium for bacteria and potato dextrose agar as medium for fungi respectively. The stock solution (10^{-2} mol L^{-1}) was prepared by dissolving the compounds in DMF and the solutions were serially diluted in order to find the minimum inhibitory concentration (MIC) values. In a usual procedure [24], a well was made on the agar medium inoculated with microorganisms. The well was filled with the test solution using a micropipette and the plates were incubated, 48 h for bacteria and 72 h for fungi at 35 $^\circ\text{C}$. During this period, the test solution was diffused and the growth of inoculated microorganisms was affected. Tetracycline and nystatin were used as standard control drugs for bacteria and fungi respectively.

DNA interaction studies: The solutions of Calf Thymus DNA (CT-DNA) in *tris*-hydrochloric acid and sodium chloride

buffer (pH = 7.2) in water with a ratio 1.9 of A_{260}/A_{280} UV absorbance, signifying that DNA was suitably liberated from protein. For 25 cycles sonicated, concentrated stock DNA solutions prepared in buffer and 30 s each cycle consistence, with minute intervals. The DNA concentration was measured by using its molar extinction coefficient at 260 nm after required dilutions. DNA stock solutions were stored at 4 °C and used within a day. Copper complexes/DNA was prepared by dissolving in alcohol and diluted with buffer solution to the requisite concentration for all the desired experiments. For absorption measurement and cyclic voltammogram experiments, the DNA solutions were pretreated with the solution of the complex to ensure no change in their concentration.

Electronic absorption spectroscopic studies: Absorption spectral titration experiments were performed by keeping the concentration of complex as constant while varying the concentration of CT-DNA. It was achieved by dissolving required amount of the copper complex and stock solutions of DNA which is sustaining the total volume as constant. This resulted in a series of solutions with varying concentrations of DNA but with constant concentration of the complex. The absorbance was measured after successive addition of CT-DNA pretreated with the complex.

Cyclic voltammetric studies: In cyclic voltammetry measurements, the freshly polished glassy carbon electrode was modified by transferring a droplet of 2 μ L of 5×10^{-3} M of CT-DNA on the surface and dried in air. Then the electrode was rinsed with distilled water. A CT-DNA modified glassy carbon electrode was used as a working electrode, Ag/AgCl as standard electrode and Pt wire as auxiliary electrode. A known concentration of freshly prepared complex solution was used to record the cyclic voltammogram and compared with cyclic voltammogram of CT-DNA – $[\text{CuL}_2]\text{Cl}_2$ complex.

RESULTS AND DISCUSSION

Physical characterization, micro analytical, molar conductance and magnetic susceptibility data of the complexes are given in Table-1.

The analytical data of the metal complexes correspond well with the general formula $[\text{ML}_2]\text{Cl}_2$ where M = Cu(II), Ni(II), Co(II), Mn(II) and Zn(II); L = $\text{C}_{21}\text{H}_{19}\text{N}_5\text{S}$. The electrolytic nature of the complexes was confirmed from their magnetic

susceptibility data. The higher conductance values of the chelates support their 1:2 electrolytic natures [25] and are consistent with other related complexes. Presence of the chloride ion is evident from the Volhard's test and that of the sulfate ion from the BaCl_2 test.

Mass spectra: FAB-Mass spectrum was clearly obtained for the Schiff base (L) and shows its characteristic molecular ion peak ($\text{C}_{21}\text{H}_{19}\text{N}_5\text{S}$) at m/z 373 $[\text{M}^+]$. Also, the FAB-Mass spectrum of $[\text{CuC}_{42}\text{H}_{38}\text{N}_{10}\text{S}_2]\text{Cl}_2$ complex which exhibits a molecular ion peak at m/z 881 $[\text{M}^+]$, which confirms the expected stoichiometry of complex as $[\text{ML}_2]\text{Cl}_2$. This is further supported by elemental analysis data of Schiff base and its complexes. Also, the entire XRD spectra had polycrystalline with good crystalline in nature.

X-ray diffraction studies: The XRD patterns of Schiff base and its $[\text{CuL}_2]\text{Cl}_2$, $[\text{MnL}_2]\text{Cl}_2$ and $[\text{ZnL}_2]\text{Cl}_2$ complexes were shown in Fig. 1. The Schiff base (Fig. 1a) shows the peaks at 10.3195° , 12.417° , 14.625° , 15.528° , 21.654° , 24.642° , 29.261° , 31.8758° , 33.19° and 42.001° suggested that it is polycrystalline structure. The 100 % intensity appears at 21.654° for Schiff base (L) and the same was observed in all the complexes indicate that the metal ion is incorporated within the ligand environment. Some new peaks were also observed in the XRD pattern of metal complexes. The peak intensity at 21.733° for $[\text{MnL}_2]\text{Cl}_2$ complex (Fig. 1c) is increased when compared to Schiff base while $[\text{CuL}_2]\text{Cl}_2$ (Fig. 1b) and $[\text{ZnL}_2]\text{Cl}_2$ (Fig. 1d) complexes is reduced. The strongest broad diffraction peaks for the above two complexes were observed at 27.928° and 31.762° respectively which suggests the quantum confinement in Schiff base by the attachment of donor atoms to metal ion in the chelates [26,27]. The decrease in intensity of these peaks in $[\text{CuL}_2]\text{Cl}_2$ and $[\text{ZnL}_2]\text{Cl}_2$ complexes represents the reduced crystalline size due to the increasing full width half maximum (FWHM) values.

The crystallite sizes were calculated for prominent peaks for the prepared Schiff base metal complexes using following Debye-Scherrer's formula:

$$D = 0.9 \frac{\lambda}{\beta \cos \theta}$$

where, λ is the wavelength of CuK_α used, β is full width at half maximum of the peak position in radian; θ is Bragg diffraction angle at peak position in degrees. The average

TABLE-1
CHARACTERIZATION OF PHYSICAL, ANALYTICAL, MOLAR CONDUCTANCE
AND MAGNETIC SUSCEPTIBILITY DATA OF METAL-CHELATES

Compound	Colour	m.p. (°C)	Elemental analysis (%): Found (calcd.)						Λ_m ($\Omega^{-1} \text{ cm}^2 \text{ mol}^{-1}$) (10^{-2})	μ_{eff} (BM)
			M	C	H	N	S	Cl		
L	Reddish brown	157	–	67.52 (67.56)	5.06 (5.09)	18.74 (18.77)	8.57 (8.58)	–	–	–
$[\text{CuL}_2]\text{Cl}_2$	Brown	324	7.17 (7.21)	57.18 (57.21)	4.27 (4.31)	15.86 (15.89)	7.24 (7.26)	8.02 (8.06)	68	1.83
$[\text{NiL}_2]\text{Cl}_2$	Brown	346	6.67 (6.70)	57.53 (57.55)	4.30 (4.34)	15.95 (15.99)	7.28 (7.31)	8.09 (8.11)	56	2.91
$[\text{CoL}_2]\text{Cl}_2$	Reddish orange	355	6.71 (6.74)	57.50 (57.53)	4.32 (4.34)	15.93 (15.98)	7.27 (7.31)	8.08 (8.11)	74	3.94
$[\text{MnL}_2]\text{Cl}_2$	Pale orange	325	6.28 (6.31)	57.78 (57.80)	4.33 (4.36)	16.02 (16.06)	7.30 (7.34)	8.11 (8.14)	86	5.98
$[\text{ZnL}_2]\text{Cl}_2$	Pale green	338	7.38 (7.41)	57.12 (57.14)	4.27 (4.31)	15.85 (15.87)	7.23 (7.26)	8.01 (8.05)	64	–

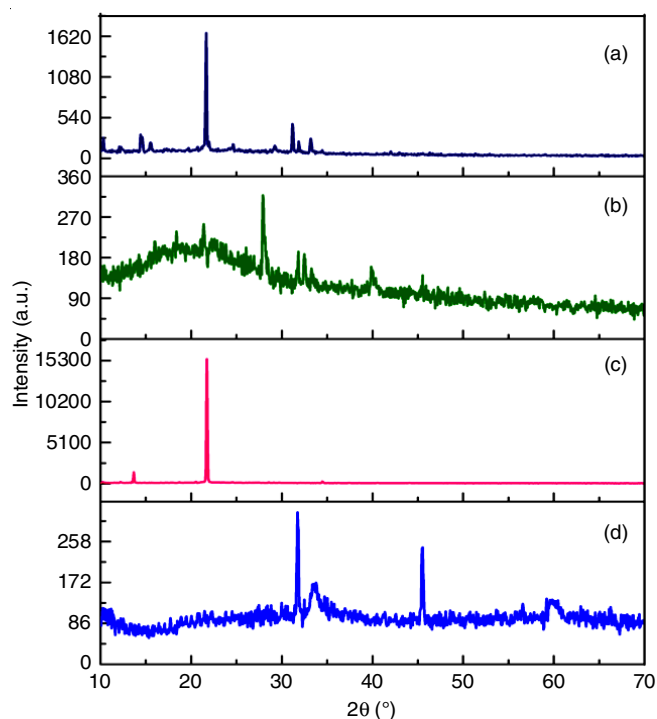


Fig. 1. Powder XRD pattern of Schiff base (a) and its $[\text{CuL}_2]\text{Cl}_2$ (b), $[\text{MnL}_2]\text{Cl}_2$ (c) and $[\text{ZnL}_2]\text{Cl}_2$ (d) complexes

crystallite size of Schiff base and its $[\text{CuL}_2]\text{Cl}_2$, $[\text{MnL}_2]\text{Cl}_2$ and $[\text{ZnL}_2]\text{Cl}_2$ complexes are 57, 56, 42 and 36 nm, respectively. The minimum crystalline size was observed for $[\text{ZnL}_2]\text{Cl}_2$ complex and it has better crystalline nature than other complexes.

Morphological study: The surface morphology of Schiff base and its complexes were studied by using scanning electron microscope (SEM). SEM images for Schiff base (a) and its $[\text{CuL}_2]\text{Cl}_2$ (b), $[\text{MnL}_2]\text{Cl}_2$ (c) and $[\text{ZnL}_2]\text{Cl}_2$ (d) complexes were shown in Fig. 2. From the SEM image of the Schiff base and its $[\text{CuL}_2]\text{Cl}_2$, $[\text{MnL}_2]\text{Cl}_2$ and $[\text{ZnL}_2]\text{Cl}_2$ complexes, irregular spherical grain structure for Schiff base, cloud like model for $[\text{CuL}_2]\text{Cl}_2$, well dispersed, heterogeneous sized with highly agglomerated grains for $[\text{MnL}_2]\text{Cl}_2$ and cauliflower model like structure for $[\text{ZnL}_2]\text{Cl}_2$ complex was observed.

Furthermore, the crystalline size of complexes was reduced when compared with ligand due to incorporation of metal ion. The minimum crystalline size was found for $[\text{ZnL}_2]\text{Cl}_2$ complex which is further supported by XRD data. The SEM image of the complexes confirms the presence of ligands in the metal-chelates. Hence, the metal ion affects the morphology of Schiff base in the metal-chelates [28-30].

IR spectra: The IR spectra provide most valuable information concerning the coordinating sites of Schiff base. A comparative study of the IR spectra of Schiff base and its metal-

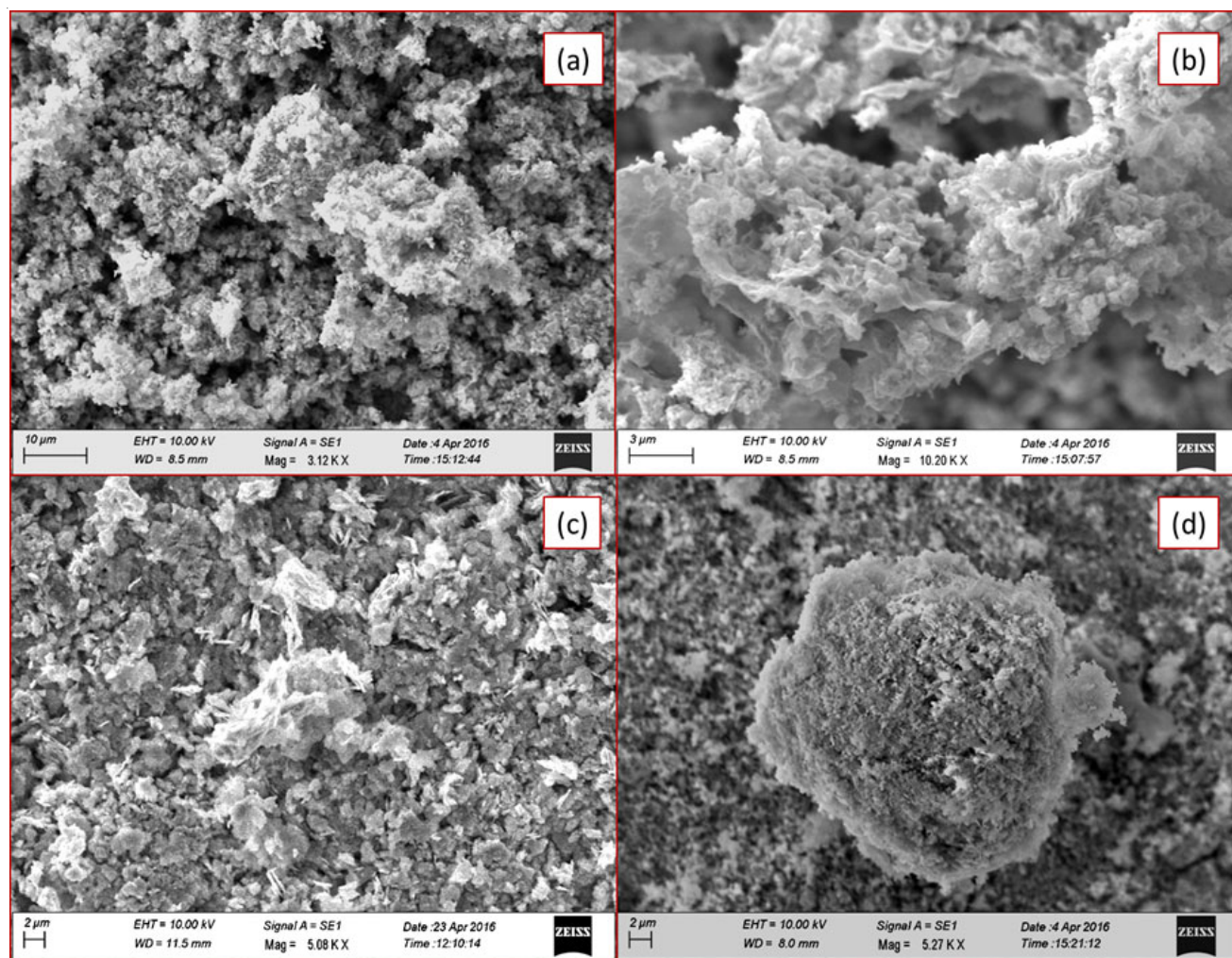


Fig. 2. SEM images for Schiff base (a) and its $[\text{CuL}_2]\text{Cl}_2$ (b), $[\text{MnL}_2]\text{Cl}_2$ (c) and $[\text{ZnL}_2]\text{Cl}_2$ (d) complexes

chelates revealed that certain peaks are common and therefore, only provides important peaks, which have been either shifted or newly appeared, are discussed. The IR spectra of the Schiff base showed that the characteristic $\nu(\text{C}=\text{N})$ bands in the 1651 cm^{-1} region which is shifted to lower frequencies in the spectra of all the metal chelates ($1645\text{--}1640\text{ cm}^{-1}$) representing the involvement of azomethine nitrogen in coordination to the metal ion [31]. The $\nu(\text{C}-\text{S})$ stretching frequency of the thiazole ring was appeared at 780 cm^{-1} and it was shifted to $775\text{--}765\text{ cm}^{-1}$ region due to chelation. This is further supported by the appearance of new bands at $518\text{--}513$ and $462\text{--}442\text{ cm}^{-1}$ region attributed to $\nu(\text{M}-\text{N})$ and $\nu(\text{M}-\text{S})$ frequencies, respectively in all the metal chelates [32].

^1H NMR spectra: The ^1H NMR spectra of Schiff base and its zinc complex were recorded in CDCl_3 solution (Fig. 3). The Schiff base exhibits the following signals: phenyl as multiplet at $7.53\text{--}7.58\text{ }\delta$, $=\text{CCH}_3$ at $2.60\text{ }\delta$, $-\text{N}-\text{CH}_3$ at $3.18\text{--}3.30\text{ }\delta$, $-\text{CH}-$ at $5.78\text{ }\delta$, $-\text{N}-\text{C}=\text{CH}$ at $7.93\text{--}8.23$ and $-\text{C}-\text{S}-\text{CH}-$ at $7.69\text{--}7.71\text{ }\delta$ (thiazole ring). A slight downfield shift was observed in all the signals in the spectrum of zinc complex clearly indicated that the coordination ligand system with metal ion.

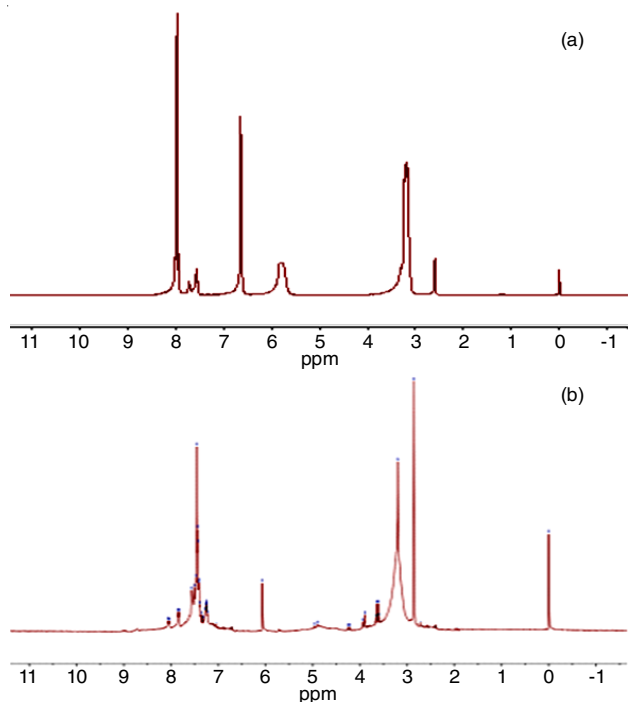


Fig. 3. ^1H NMR Spectra of Schiff base (a) and $[\text{ZnL}_2]\text{Cl}_2$ complex (b) in CDCl_3 solution.

Electronic absorption spectra: The electronic absorption spectra can regularly provide quick and reliable information about the ligand arrangement in metal complexes. It is also serves as a useful tool to distinguish among the square-planar, square-pyramidal, tetrahedral and octahedral geometries of the complexes. The absorptions in the ultraviolet region are attributed to transitions within the ligand orbital and those in the visible region are probably due to allowed metal-to-ligand charge transfer transitions.

The ligand (L) in MeCN shows an absorption bands at about 248 nm and 304 nm which are assigned as intraligand charge transfer bands. The UV-visible spectrum of $[\text{CuL}_2]\text{Cl}_2$

complex in acetonitrile shows three bands which are assigned as an intraligand charge transfer bands (236 nm and 308 nm) and a $d-d$ band ($^2\text{E}_g \rightarrow ^2\text{T}_{2g}$), (702 nm). The $d-d$ band (668 nm) strongly favours octahedral geometry around the metal ion. This is further supported by the magnetic susceptibility value (1.83 BM).

The $[\text{NiL}_2]\text{Cl}_2$ complex in MeCN solution shows three $d-d$ bands at 786 , 690 and 553 nm which are assigned as $^3\text{A}_{2g}(\text{F}) \rightarrow ^3\text{T}_{2g}(\text{F})$, $^3\text{A}_{2g}(\text{F}) \rightarrow ^3\text{T}_{1g}(\text{F})$ and $^3\text{A}_{2g}(\text{F}) \rightarrow ^3\text{T}_{1g}(\text{P})$ transitions, respectively. The appearance of a band in the near IR region (786 nm) is characteristic for octahedral geometry. This is also confirmed by the magnetic susceptibility value (2.91 BM). It also shows two intra-ligand charge transfer (INCT) band at 242 and 298 nm .

The $[\text{CoL}_2]\text{Cl}_2$ complex in MeCN shows two strong absorption peaks at 267 nm , 298 nm UV region which are assigned as INCT bands. It also shows three absorption peaks at visible region around 495 , 698 and 772 nm which are designated as $^4\text{T}_{1g}(\text{F}) \rightarrow ^4\text{T}_{2g}(\text{F})$, $^4\text{T}_{1g}(\text{F}) \rightarrow ^4\text{A}_{2g}(\text{F})$ and $^4\text{T}_{1g}(\text{F}) \rightarrow ^4\text{T}_{1g}(\text{P})$ $d-d$ transitions respectively. A characteristic band at 772 nm confirms the existence of cobalt ion in the octahedral environment. The magnetic susceptibility value (3.93 BM) also supports this geometry [33].

Electrochemical behaviour: The cyclic voltammogram of $[\text{CuL}_2]\text{Cl}_2$ complex in MeCN solution at 300 K shown in Fig. 4.

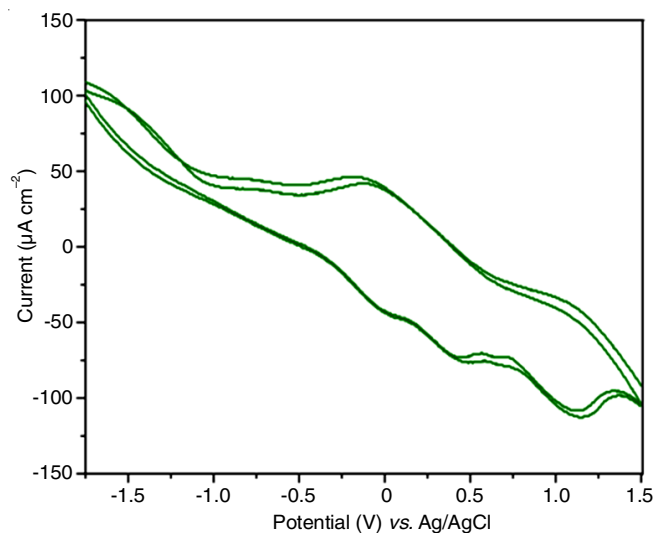
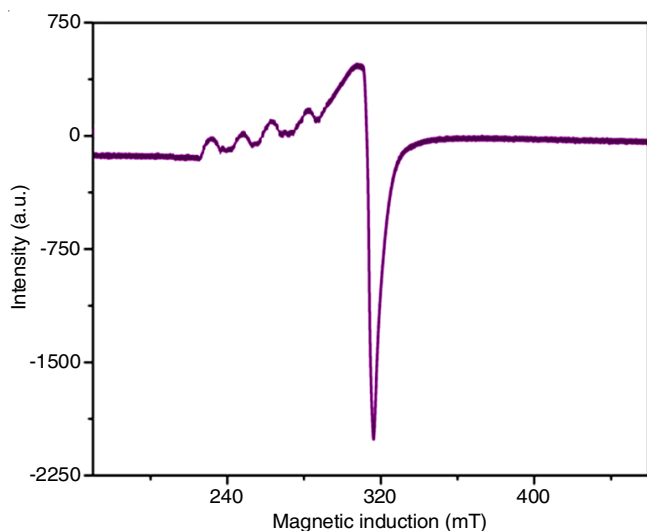


Fig. 4. Cyclic voltammogram of $[\text{CuL}_2]\text{Cl}_2$ complex in MeCN at 300 K (0.1 M TBAP) scan rate 100 mV s^{-1}

It shows two reduction peaks for $\text{Cu(II)} \rightarrow \text{Cu(I)}$ at $E_p = -0.09\text{ V}$ and $\text{Cu(I)} \rightarrow \text{Cu(0)}$ at $E_p = +1.11\text{ V}$ in the cathodic region. The corresponding oxidation peaks were observed in the anodic region at $E_p = 1.13\text{ V}$ for $\text{Cu(0)} \rightarrow \text{Cu(I)}$ and $E_p = 0.41\text{ V}$ for $\text{Cu(I)} \rightarrow \text{Cu(II)}$ with respect to Ag/AgCl electrode. A single electron transfer takes place in all the peaks based on their I_p/I_p ratio. The difference between the anodic and cathodic peaks for both couples are very high which indicates the higher stability of electrochemically generated Cu(I) and Cu(0) ionic species under experimental condition [34].

EPR spectral study: The EPR spectra of the $[\text{CuL}_2]\text{Cl}_2$ complex was recorded in DMSO at 77 K and is shown in Fig. 5.

Fig. 5. EPR spectrum of $[\text{CuL}_2]\text{Cl}_2$ complex at 77 K in DMSO solution

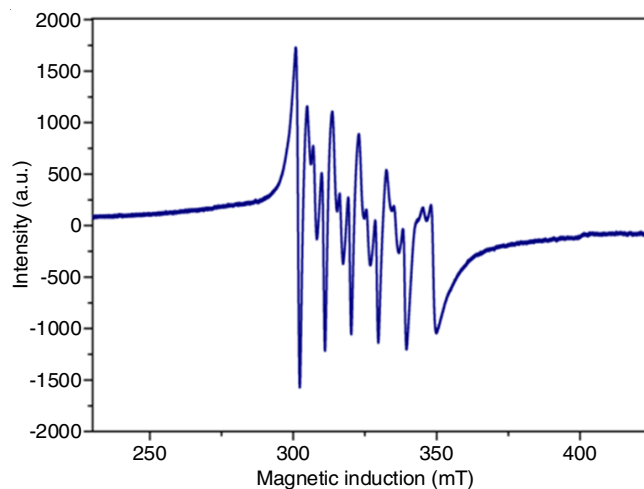
The observed spin Hamiltonian parameters values A_{\parallel} ($151 \times 10^{-4} \text{ cm}^{-1}$) $> A_{\perp}$ ($71 \times 10^{-4} \text{ cm}^{-1}$); g_{\parallel} (2.31) $> g_{\perp}$ (2.075) > 2 ensures that the system coincides well with axially elongated octahedral geometry [35,36] and the unpaired electron occupies in $d_{x^2-y^2}$ orbital. The exchange interaction parameter for the copper complex ($G = 4.13$) indicates that there is no substantial exchange interaction between copper ions.

The molecular orbital coefficients *viz.*, in-plane σ -bonding ($\alpha^2 = 0.7983$), in-plane π -bonding ($\beta^2 = 0.9158$) and out-plane π -bonding ($\gamma^2 = 0.8232$) value indicates that the presence of substantial interaction in the in-plane σ -bonding (α^2) while in-plane π -bonding (β^2) is almost ionic. This fact also suggests that there is no appropriate ligand orbital contribution in the d_{xy} orbital of copper ion. Furthermore, out-plane π -bonding is more covalent than the in-plane π -bonding. This is further supported by orbital reduction factors K_{\parallel} and K_{\perp} . They were calculated from the simplified expressions: $K_{\parallel}^2 = \alpha^2\beta^2$ and $K_{\perp}^2 = \alpha^2\gamma^2$. Significant information about the nature of the bonding in the complex can be derived from the relative magnitudes of K_{\parallel} and K_{\perp} . In case of pure s -bonding $K_{\parallel} = K_{\perp}$, whereas $K_{\parallel} < K_{\perp}$ implies considerable in-plane π -bonding, while for out-of-plane π -bonding $K_{\parallel} > K_{\perp}$. For the present copper complex K_{\parallel} (0.7310) $> K_{\perp}$ (0.6523), suggesting predominant out-plane π -bonding while the in-plane π -bonding is weaker.

The X-band ESR spectrum of $[\text{MnL}_2]\text{Cl}_2$ complex in DMSO solution was recorded at 77 K and is given in Fig. 6.

It shows a six-line hyperfine splitting due to Mn(II) ($I = 5/2$) ion. The spin Hamiltonian parameters of $[\text{MnL}_2]\text{Cl}_2$ complex in DMSO solution at 77 K ($A_{\text{iso}} = 110 \times 10^{-4} \text{ cm}^{-1}$ and $g_{\text{iso}} = 1.99 < 2$) are similar to those of mono nuclear hexa-coordinate manganese complexes with ground state $^6S_{5/2}$, indicates that there is no significant magnetic interaction between the manganese(II) ions. This fact is also supported by the magnetic susceptibility data of the complexes [37,38].

Thermogravimetric analysis: Thermal analysis plays an important role in the study of physico-chemical behaviours and of decomposition, being unaffected at below about 150 °C and 150-220 °C. It indicates the absence of water molecules in both coordination sphere and ionization sphere [39]. The

Fig. 6. ESR spectrum of $[\text{MnL}_2]\text{Cl}_2$ complex at 77 K in DMSO solution

anhydrous complexes remained stable ranges among 220-400 °C and subsequently showed rapid degradation due to decomposition of the organic constituents of the complexes. The decomposition continued up to about 700 °C and a stable product (as oxide) was formed as indicated by consistency in weight in the plateau of the thermogram.

DNA-Absorption spectral titration: The positive synergistic results were obtained from the antimicrobial studies are encouraged to investigate the interaction between DNA and copper complex. Absorption spectral titration is an important technique to find out binding mode and binding affinity of synthesized compounds with CT-DNA [40]. Absorption spectra of copper complex in presence and absence of DNA in Tris-HCl buffer (pH 7.0) are shown in Fig. 7.

Upon addition of DNA increases to $[\text{CuL}_2]\text{Cl}_2$ complex, the peak intensity changes arise in the intra-ligand charge transfer band (INCT) at 244 and 281 nm. As a result shows that, the hypochromism (46.53 %) with red shift (5.5 nm) was observed. These spectral characteristics suggest that, $[\text{CuL}_2]\text{Cl}_2$ complex interact with DNA *via* stacking interaction between the aromatic chromophore of the ligand through intercalative mode and the base pairs of DNA [41]. Moreover, the binding affinity (K_b) of $[\text{CuL}_2]\text{Cl}_2$ complex (6.424×10^3) is lower than classical intercalator (Ethidium bromide 1.4×10^6). The DNA binding of metal complexes have well established to narrate antimicrobial studies.

Cyclic voltammogram of $[\text{CuL}_2]\text{Cl}_2$ complex with DNA were recorded at 300 K in the presence and absence of DNA in Tris-HCl buffer (pH 7.2) are shown in Fig. 8. It shows a direction reduction peak at $E_p = 0.015 \text{ V}$ for $\text{Cu(II)} \rightarrow \text{Cu(I)}$ and $E_p = 0.98 \text{ V}$ for $\text{Cu(I)} \rightarrow \text{Cu(0)}$ in the cathodic regions. At anodic side, oxidation peak was observed at $E_p = 0.87 \text{ V}$ [$\text{Cu(0)} \rightarrow \text{Cu(I)}$] and $E_p = -0.022 \text{ V}$ [$\text{Cu(I)} \rightarrow \text{Cu(II)}$] regions. It reveals that the cyclic voltammogram pattern of $[\text{CuL}_2]\text{Cl}_2$ complex was totally altered due to strong binding of CT-DNA.

Antimicrobial assays: An *in vitro* antimicrobial activity results of the Schiff base metal complexes was tested against the three Gram-negative (*Escherichia coli*, *Klebsiella pneumonia* and *Salmonella typhi*) and two Gram-positive (*Staphylococcus aureus* and *Bacillus subtilis*) bacterial strains and for *in vitro* antifungal activity against *Candida albicans*, *Rhizoctonia*

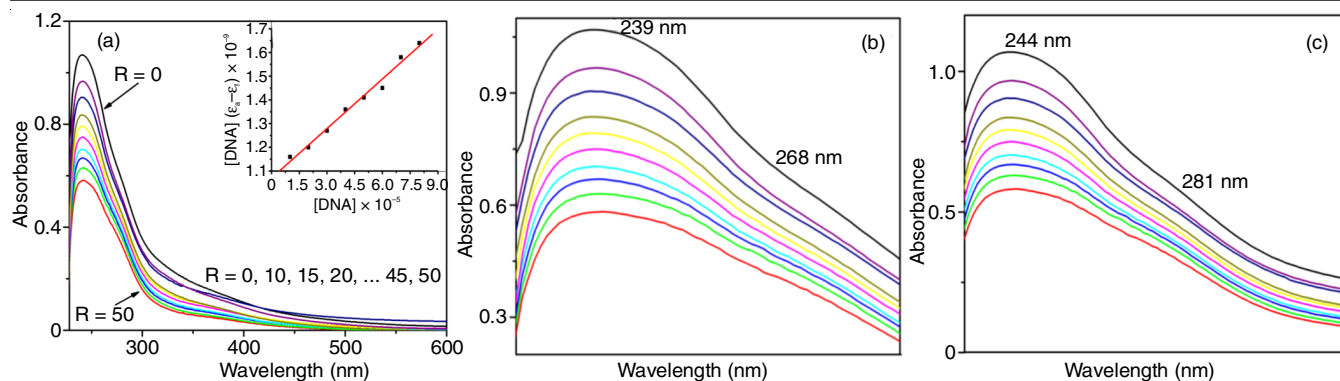


Fig. 7. Absorption spectra (a) of $[\text{CuL}_2]\text{Cl}_2$ complex (1×10^{-5} M) in presence and absence of increasing amounts of CT-DNA (0 – 50×10^{-3} M). Inset: Linear plot of $[\text{DNA}]/(\epsilon_0 - \epsilon_\infty)$ versus $[\text{DNA}]$ for the titration of DNA with $[\text{CuL}_2]\text{Cl}_2$ complex. For ligand peaks (b) and $[\text{CuL}_2]\text{Cl}_2$ complex bound peaks (c) at room temperature in 50 mM Tris-HCl/NaCl buffer (pH = 7.2)

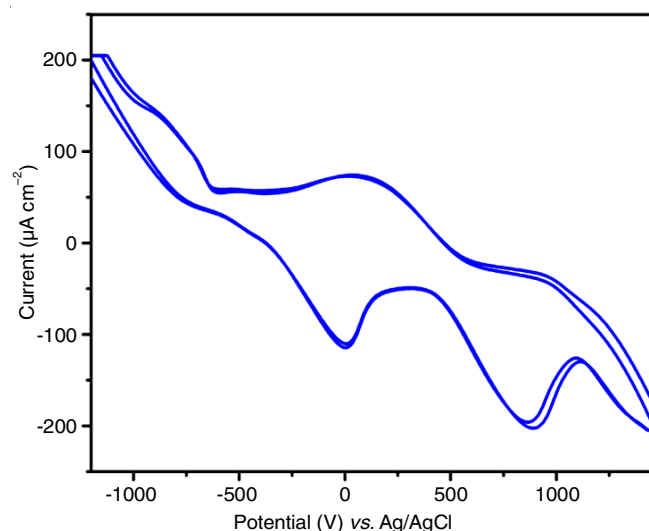


Fig. 8. Cyclic voltammogram of $[\text{CuL}_2]\text{Cl}_2$ complex with DNA in Tris-HCl buffer at 300 K Scan rate 100 mV/s

bataicola, *Aspergillus flavus*, *Aspergillus niger* and *Rhizopus stolonifer* by disc diffusion method.

The values of minimum inhibitory concentration (MIC) of Schiff base transition metal-chelates are summarized in Tables 2 and 3. A comparative study of Schiff base (L) and its metal-chelates (MIC values) indicate that metals exhibit higher antimicrobial activity than Schiff base (free ligand) which is shown in Fig. 9(a). From the MIC values, it was found that the $[\text{CuL}_2]\text{Cl}_2$ and $[\text{ZnL}_2]\text{Cl}_2$ were somewhat more potent among the other investigated Schiff base metal-chelates.

Overtone's concept [42] and Tweedy's chelation theory [43], revealed that such increased activity results of the complexes have explained clearly by the researchers using the different micro-organisms. The lipid membrane that surrounds the cell positive discrimination route only the lipid-soluble resources due to which liposolubility is a significant factor, which controls the anti-fungal activity results by overtone's theory of cell permeability.

The metal ion polarity have reduced to a larger extent due to the overlap of Schiff base orbital and partial sharing of the positive charge of the metal ion with donor groups on chelation effects. Besides, it increases delocalization of π -electrons over the entire chelate rings and better enhanced

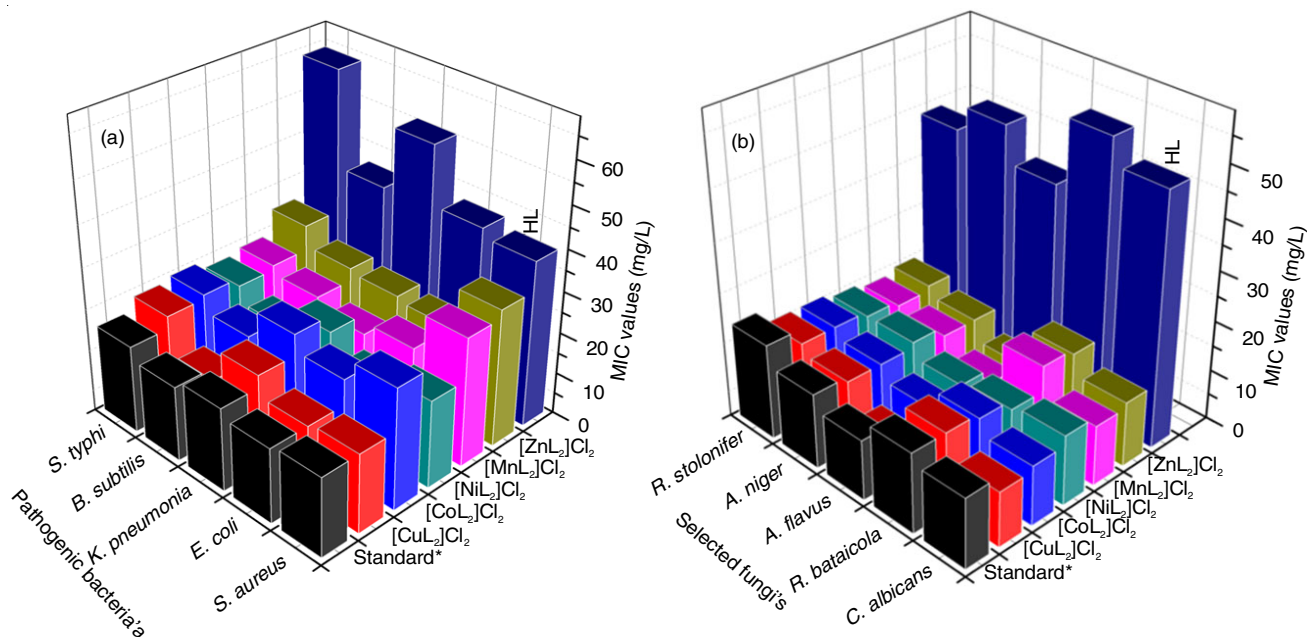


Fig. 9. Minimum inhibitory concentration (MIC) values of the synthesized compounds against the growth of bacteria's (a) and fungi's (b)

TABLE-2
ANTIBACTERIAL ACTIVITY OF THE SCHIFF BASE AND ITS METAL-CHELATES (MIC VALUE IN mg/L)

Compound	Minimum inhibitory concentration (mg/L)				
	<i>Staphylococcus aureus</i>	<i>Escherichia coli</i>	<i>Klebsiella pneumonia</i>	<i>Bacillus subtilis</i>	<i>Salmonella typhi</i>
L	40	42	56	41	64
[CuL ₂]Cl ₂	19	18	23	15	24
[CoL ₂]Cl ₂	29	24	28	21	25
[NiL ₂]Cl ₂	21	18	24	19	23
[MnL ₂]Cl ₂	31	22	19	22	24
[ZnL ₂]Cl ₂	33	23	24	25	30
Tetracycline (Standard)	19	18	20	18	21

TABLE-3
ANTIFUNGAL ACTIVITY OF THE SCHIFF BASE AND ITS METAL-CHELATES (MIC VALUE IN mg/L)

Compound	Minimum inhibitory concentration (mg/L)				
	<i>C. albicans</i>	<i>R. bataicola</i>	<i>A. flavus</i>	<i>A. niger</i>	<i>R. stolonifer</i>
L	50	55	42	49	44
[CuL ₂]Cl ₂	11	16	8	14	16
[CoL ₂]Cl ₂	12	15	11	14	16
[NiL ₂]Cl ₂	14	13	12	15	15
[MnL ₂]Cl ₂	12	18	9	13	14
[ZnL ₂]Cl ₂	13	17	9	13	15
Nystatin (Standard)	14	16	12	15	19

lipophilicity of metal-chelates in Fig. 9(b). This kind of increased lipophilicity enhances the penetration of metal-chelates into lipid membranes and blocking of the metal binding sites in the enzymes of microorganisms. Besides, the mode of action of the compounds could involve the formation of a hydrogen bond through the azomethine group with the active centre of cell constituents, ensuing in interferences with the normal cell process. Moreover, it disturbs the respiration process of the cell and accordingly blocks the synthesis of the proteins that restricts further growth of the organisms [44,45].

Conclusion

Cationic Cu(II), Ni(II), Co(II), Mn(II) and Zn(II) complexes have been synthesized from the Schiff base derived from benzylidene-4-imino-2,3-dimethyl-1-phenyl-3-pyrazolin-5-one and 2-aminothiazole. The synthesized compounds were characterized by microanalytical data, FAB-Mass spectra, Powder XRD, SEM, FTIR, UV-visible, ¹H NMR, EPR, CV and thermal analysis techniques. The analytical data and FAB-Mass of the complexes give the general formula as [ML₂]Cl₂. Powder XRD data and SEM images ensure that the complexes are nano size grain with good polycrystalline structure and crystalline nature. The magnetic susceptibility and electronic absorption spectra of the complexes indicate that all the complexes exhibit the octahedral geometry around the central metal ion. The observed ESR parameters clearly suggest that the complex is axially elongated octahedral geometry. DNA interaction studies of [CuL₂]Cl₂ complex using electronic absorption spectra and cyclic voltammogram measurements revealed that the binding occurs through intercalation between [CuL₂]Cl₂ complex and CT-DNA. The *in vitro* biological screening effects of the investigated compounds were tested against various bacteria and fungi. The minimum inhibitory concentration values indicate that most of the complexes have higher toxicity than the ligand against the microorganisms.

ACKNOWLEDGEMENTS

The authors thank The Principal and Dr. A. Cyril, Head, Department of Chemistry, Raja Doraisingam Government Arts College for providing the necessary research facilities. Thanks are also due to Dr. S. Viswanathan, School of Industrial Chemistry, Alagappa University, Karaikudi, India for cyclic voltammetry and cyclic voltammetry-DNA facilities; The Head, School of Chemistry, Madurai Kamaraj University, Madurai, India (NMR facilities), The Head, Madura College, Madurai, India; Dr. A. Nagendran, Assistant Prof., Alagappa Government Arts College, Karaikudi (IR and UV-visible-DNA facilities) and the Head, SAIF, IIT, Mumbai for providing spectral and analytical data facilities.

REFERENCES

1. J.S. Kumaran, S. Priya, J. Muthukumaran, N. Jayachandramani and S. Mahalakshmi, *J. Chem. Pharm. Res.*, **5**, 56 (2013).
2. P. Deshmukh, P.K. Soni, A. Kankoriya, A.K. Halve and R. Dixit, *Int. J. Pharm. Sci. Rev. Res.*, **34**, 26, 162 (2015).
3. J.S. Kumaran, S. Priya and J. Gowsika, *Res. J. Pharm. Biol. Chem. Sci.*, **4**, 279 (2013).
4. M.N. Al-Jibouri, F.R. Hafith and A.M. Rasheed, *Eur. Chem. Bull.*, **3**, 559 (2014); <https://doi.org/10.17628/ecb.2014.3.559-562>.
5. M. Noroozifar, M. Khorasani-Motlagh and P.A. Fard, *Eur. J. Med. Chem.*, **45**, 5438 (2010); <https://doi.org/10.1016/j.ejmech.2010.09.004>.
6. P. Goel, D. Kumar and S. Chandra, *J. Chem. Biol. Phys. Sci.*, **4**, 1946 (2014).
7. T. Ahmad, F. Kandil and C. Moustaph, *AASCIT Commun.*, **2**, 127 (2015).
8. H.L. Siddiqui, A. Iqbal, S. Ahmad and G.W. Weaver, *Molecules*, **11**, 206 (2006); <https://doi.org/10.3390/11020206>.
9. A.-N.M.A. Alaghaz and H.A. Bayoumi, *Int. J. Electrochem. Sci.*, **8**, 11860 (2013).
10. L.H. Abdel-Rahman, R.M. El-Khatib, L.A.E. Nassr, A.M. Abu-Dief, F.E. Lashin, *Spectrochim Acta A: Mol. Biomol. Spectrosc.*, **111**, 266 (2013); <https://doi.org/10.1016/j.saa.2013.03.061>.

11. T. Arun, R. Subramanian and N. Raman, *J. Photochem. Photobiol. B*, **154**, 67 (2016); <https://doi.org/10.1016/j.jphotobiol.2015.11.011>.
12. X. Zhou, L. Shao, Z. Jin, J.-B. Liu, H. Dai, J.-X. Fang, *Heteroatom Chem.*, **18**, 55 (2007); <https://doi.org/10.1002/hc.20256>.
13. A.M. Nalawade, R.A. Nalawade, S.M. Patange and D.R. Tase, *Int. J. Eng. Sci. Invention*, **2**, 2319 (2013).
14. W. Al Zoubi, *Int. J. Org. Chem.*, **3**, 73 (2013); <https://doi.org/10.4236/ijoc.2013.33A008>.
15. A.M. Abu-Dief and I.M.A. Mohamed, *Beni-Suef Univ. J. Basic Appl. Sci.*, **4**, 119 (2015); <https://doi.org/10.1016/j.bjbas.2015.05.004>.
16. M.A. Neelakantan, M. Esakkiammal, S.S. Mariappan, J. Dharmaraja and T. Jeyakumar, *Indian J. Pharm. Sci.*, **72**, 216 (2016); <https://doi.org/10.4103/0250-474X.65015>.
17. N. Revathi, M. Sankarganesh, J. Rajesh and J.D. Raja, *J. Fluoresc.*, **27**, 1801 (2017); <https://doi.org/10.1007/s10895-017-2118-y>.
18. F.C. Jiang and C.Y. Cheng, *Yao Xue Xue Bao*, **41**, 727 (2006).
19. A.M. Katsori, M. Chatzopoulou, C. Kontogiorgis, A. Patsilinos, K. Dimas, T. Trangas and D. Hadjipavlou-Litina, *Eur. J. Med. Chem.*, **46**, 2722 (2011); <https://doi.org/10.1016/j.ejmech.2011.03.060>.
20. J. Lal, S.K. Gupta, D. Thavaselvam and D.D. Agarwal, *Eur. J. Med. Chem.*, **64**, 579 (2013); <https://doi.org/10.1016/j.ejmech.2013.03.012>.
21. J.E. Dickson and L.A. Summers, *Aust. J. Chem.*, **23**, 1023 (1970); <https://doi.org/10.1071/CH9701023>.
22. D.D. Perrin, W.L.F. Armarego and D.R. Perrin, *Purification of Laboratory Chemicals*, Oxford, UK: Pergamon Press (1980).
23. R.J. Angelici, *Synthesis and Techniques in Inorganic Chemistry*, W.B. Saunders Company (1969).
24. E.C.S. Chan, M.J. Pelczar Jr. and N.R. Krieg, *Microbiology*, Tata McGraw-Hill Education Pvt. Ltd., edn 5, pp. 687-688 (1998).
25. N. Raman, R. Jeyamurugan, A. Sakthivel and L. Mitu, *Spectrochim. Acta A Mol. Biomol. Spectrosc.*, **75**, 88 (2010); <https://doi.org/10.1016/j.saa.2009.09.047>.
26. E.K. Barefield, G.M. Freeman and D.G. Van Derveer, *Inorg. Chem.*, **25**, 552 (1986); <https://doi.org/10.1021/ic00224a033>.
27. N. DeVries and J. Reedijk, *Inorg. Chem.*, **30**, 3700 (1991); <https://doi.org/10.1021/ic00019a026>.
28. N. Raman and R. Jeyamurugan, *J. Coord. Chem.*, **62**, 2375 (2009); <https://doi.org/10.1080/00958970902825195>.
29. N. Raman, R. Jeyamurugan, S. Sudharsan, K. Karuppasamy and L. Mitu, *Arab. J. Chem.*, **6**, 235 (2013); <https://doi.org/10.1016/j.arabjc.2012.04.010>.
30. E.I. Solomon, J.W. Hare and H.B. Gray, *Proc. Natl. Acad. Sci. USA*, **73**, 1389 (1976); <https://doi.org/10.1073/pnas.73.5.1389>.
31. N. Kitajima, ed: A.G. Sykes, *Advances in Inorganic Chemistry*, Academic Press, New York (1992).
32. R.K. Ray and G.B. Kauffman, *Inorg. Chim. Acta*, **173**, 207 (1990); [https://doi.org/10.1016/S0020-1693\(00\)80215-7](https://doi.org/10.1016/S0020-1693(00)80215-7).
33. N. Raman and R. Jeyamurugan, *J. Coord. Chem.*, **62**, 2375 (2009); <https://doi.org/10.1080/00958970902825195>.
34. J.K. Barton, A.T. Danishefsky and J.M. Goldberg, *J. Am. Chem. Soc.*, **106**, 2172 (1984); <https://doi.org/10.1021/ja00319a043>.
35. C.J. Dhanaraj and M.S. Nair, *J. Coord. Chem.*, **62**, 4018 (2009); <https://doi.org/10.1080/00958970903191142>.
36. A. Thakar, K. Joshi, K. Pandya and A. Pancholi, *E-J. Chem.*, **8**, 1750 (2011); <https://doi.org/10.1155/2011/282061>.
37. N. Raman, R. Jeyamurugan, R.U. Rani, T. Baskaran and L. Mitu, *J. Coord. Chem.*, **63**, 1629 (2010); <https://doi.org/10.1080/00958972.2010.485643>.
38. V. Prakash and M.S. Suresh, *Res. J. Pharm. Biol. Chem. Sci.*, **4**, 1536 (2013).
39. N. Dharmaraj, P. Viswanathamurthi and K. Natarajan, *Transition Met. Chem.*, **26**, 105 (2001); <https://doi.org/10.1023/A:1007132408648>.
40. M.M. Ali, M. Jesmin, M.S. Salahuddin, M.R. Habib and J.A. Khanam, *Int. J. Biol. Chem. Sci.*, **2**, 292 (2008); <https://doi.org/10.4314/ijbcs.v2i3.39748>.
41. Z. Tohidian, I. Sheikhshoae and M. Khaleghi, *Int. J. Nanodimens.*, **7**, 127 (2016); <https://doi.org/10.7508/IJND.2016.02.004>.
42. N. Raman, A. Kulandaisamy and K. Jeyasubramanian, *Synth. React. Inorg. Met.-Org. Chem.*, **32**, 1583 (2002); <https://doi.org/10.1081/SIM-120015081>.
43. L.H. Abdel-Rahman, R.M. El-Khatib, L.A.E. Nassr and A.M. Abu-Dief, *Arab. J. Chem.*, **10**, 1835 (2017); <https://doi.org/10.1016/j.arabjc.2013.07.010>.
44. N. Raman, A. Kulandaisamy and K. Jeyasubramanian, *Synth. React. Inorg. Met.-Org. Chem.*, **31**, 1249 (2001); <https://doi.org/10.1081/SIM-100106862>.
45. N. Raman, R. Jeyamurugan and J. Joseph, *J. Iranian Chem. Res.*, **3**, 83 (2010).